

Sivakumar C.

Assistant Professor
B. S. Abdur Rahman Crescent Institute of
Science and Technology
Department of Mechanical Engineering
India

Muralidharan V.

Associate Professor
B. S. Abdur Rahman Crescent Institute of
Science and Technology
Department of Mechanical Engineering
India

Ravikumar N.

Assistant Professor
B. S. Abdur Rahman Crescent Institute of
Science and Technology
Department of Mechanical Engineering
India

Murali Manohar D.

Assistant Professor
B. S. Abdur Rahman Crescent Institute of
Science and Technology
Department of Polymer Engineering
India

Investigations on the Mechanical and Damping Properties of Styrene-Butadiene Rubber with Graphene and Carbon Black

An experimental and numerical study on the mechanical and damping properties of styrene-butadiene rubber (SBR) composites with graphene nanoparticles (GNP) and carbon black (CB) is presented in this paper. The composites were tested for mechanical properties such as hardness and tensile strength. It is observed that the composites with GNP & CB fillers have higher stiffness and percentage elongation for failure. A scale model of the chassis was subjected to forced vibration to find the damping properties of each of the prepared composites. The experimental results were used to create a numerical model in ANSYS software using Yeoh's hyper-elastic model to generate a hyper-elastic material to simulate the composite property and to perform harmonic response analysis in ANSYS. The results from experiments and theoretical findings exhibited good agreement.

Keywords: Nanocomposites, Graphene, Hyper-Elastic Model, Viscoelastic Damping, Harmonic Response.

1. INTRODUCTION

In engineering, vibrations are essential. In applications requiring controlled vibrations, they can be reduced through balancing or using a damping layer. Rubber, with its viscoelastic nature and high loss factor, is commonly tested and employed for effective vibration absorption. Adding fillers to rubbers is a conventional method to enhance composite properties, supported by various literature. Due to the obviously improved qualities attributable to the presence of multifunctional graphene-based nanofillers, the possibilities, and capacities of graphene for advanced engineering applications are nearly limitless [1]. An increase in strength, compression resistance, and hardness in SBR/NBR as a result of adding CB is reported in [2] and quoted high cross-linking density as a reason behind it. Cross-linking degrees of vulcanizates increased with an increase in carbon nanotubes (CNT), resulting in higher storage modulus of SBR composites [3]. The oxidation degree of graphene oxide in SBR & carboxylated acrylonitrile butadiene rubber (XNBR) had a direct effect on the mechanical strength and thermal conductivity [4]. The inclusion of CNT in SBR improved the rigidity of the composite, which in turn increased the storage modulus of the material [5]. And comparatively, the effect of CB on the same material was lesser. Enhancement of tensile properties was reported when using graphene oxide (GO) on rubber composite [6-8]. Improvement in mechanical properties was presented when polyvinylpyrrolidone-modified GO was used in SBR [9], and the

synergistic effect between silica and GO in SBR [10] was significant. SBR/ natural rubber (NR) with cellulose nanocrystal (CNC) and graphene exhibited increased storage modulus and tribological properties [11]. Conductive carbon black had a maximum effect on the hardness and tensile strength of ethylene-propylene-diene rubber (EPDM) when compared to other structures of carbon black [12]. The industrial carbon black had a lesser impact than pyrolytic carbon black (pCB) N330 on SBR, with stronger tear strength and higher tensile strength [13]. The effect of nanofillers on nitrile rubber/polyvinyl chloride (NBR/PVC) (50:50) rubber was studied for tensile and hardness properties and reported that GNP has the upper hand in enhancing the base rubber when compared to organically modified montmorillonite (OMMT) nano clay [14,15].

Viscoelastic materials are widely employed in energy-absorbing elements in many technical applications such as automotive, aerospace, and military [16]. Damping characteristics of silica-filled SBR/BR were studied using a dynamic mechanical analyzer (DMA), and it was found that the loss factor was higher at lower frequencies and decreasing trend at higher frequencies with an increase in styrene loading. The viscoelastic property of the composite was validated analytically using the Maxwell-Weichast model [17]. Free vibration test and corresponding theoretical validation were conducted to find damping properties of hybrid composites containing glass fiber which had 44% more loss modulus than the composite with carbon fiber [18]. Forced and free vibration tests on CNT-epoxy composites for structural vibration applications emphasizing damping and stiffness properties are given [19]. Significant improvement in structural damping and dynamic viscoelastic loss is reported in OMMT-filled nitrile rubber/polyvinyl chloride (NBR-PVC) 70/30

Received: April 2023, Accepted: June 2023

Correspondence to: Muralidharan V, Department of Mechanical Engineering, B. S. Abdur Rahman Crescent Institute of Science and Technology, Chennai, India.

E-mail: muralidharan@crescent.education

doi: 10.5937/fme2303386C

© Faculty of Mechanical Engineering. All rights reserved

FME Transactions (2023) 51, 386-395 386

(w/w) nanocomposites. Aluminum beam vibration damping in a constrained layer damping (CLD) revealed that NVC73-5OMMT produced reliably high damping at all modal frequencies and emphasized that it might be caused by improved exfoliation and uniform clay dispersion in the matrix [20]. The loss factor of hybrid structures and laminates containing viscoelastic materials with experimental and numerical calculations was reported [21-24]. The influence of black carbon structure with the same volume fraction on mechanical and vibration damping characteristics has been studied [25], and it observed that smaller particle size of carbon black increased the stiffness of the rubber along with hardness, and the forced oscillation test showed that larger particles lead to improved vibrational damping. The data from the DMA and high-frequency dynamic mechanical analyzer (HFDMA) test of SBR-CB was used to get viscoelastic properties at high frequencies using General Maxwell Mode (GMM), which will eliminate the need for using DMA and Williams, Landel, and Ferry (WLF) relation [26]. To predict the vibration response of viscoelastic material, it is necessary to study both viscous damping and viscoelastic material damping [27]. A reliable way to determine the damping loss factor for viscoelastic material, which is unaffected by excitation force, shape, and substance, is reported [28] and validated using finite element analysis. Thin plies of carbon fiber in Methylmet-hacrylate (MMA) resin helped in increasing loss modulus and loss factor in comparison with epoxy composite [29].

A different approach to finite element analysis of composite materials to predict structural behavior is reported [30-34].

The existing studies on vibration damping and isolation have primarily focused on characterizing and theoretically modeling viscoelastic materials. However, there is a scarcity of research on the practical implementation of SBR nanocomposites as vibration isolation materials, specifically motor mounts. Consequently, this current work represents an initial endeavor toward examining the applicability of SBR composites as vibration mounts for effectively isolating motor vibrations in real-world applications.

This paper focuses on the effect of different volume concentrations of carbon black and graphene in SBR on mechanical and damping properties. The prepared samples were subjected to tensile and vibration tests. Subsequently, the results were validated using a hyperelastic material model and harmonic response analysis using ANSYS software.

2. EXPERIMENTAL PROCEDURE

2.1 Materials

Styrene Butadiene Rubber (Relflex Stylamer SBR 1712, referred to as SBR) was supplied by Relflex Elastomers, Chennai, India. It consists of 23.5% bound Styrene. High Abrasion Furnace Carbon black (referred to as CB) N326 of the average agglomerate size of 2–5 μm was obtained from Birla Carbon India Pvt. Ltd., Chennai, India.

The graphene powder (also known as GPN) was purchased from Adnano Technologies, Karnataka,

India, and used as received. It had an average thickness (Z) of 3-8 nm, an average lateral dimension (X and Y) of 5-10 μm , and a surface area of 180 m^2/g with 3-6 layers. Additional ingredients, including zinc oxide (ZnO), stearic acid, Tetramethyl thiuram disulfide (TMTD), and sulfur, were used without any changes.

2.2 Sample Preparation

The experiment was carried out on the SBR, a synthetic rubber made of styrene and butadiene, known for their good abrasion resistance properties. The samples were made into blank SBR for reference and 10 & 20 phr of each GNP and CB according to the composition shown in Table 1.

Table 1. Composition ratio

Ingredients phr*	Samples				
	SBR Blank	SBR 10 CB	SBR 20 CB	SBR 10 GNP	SBR 20 GNP
SBR	100	100	100	100	100
Stearic Acid	1	1	1	1	1
ZnO	5	5	5	5	5
TMTD	1.5	1.5	1.5	1.5	1.5
Sulfur	1.5	1.5	1.5	1.5	1.5
CB	0	10	20	0	0
GNP	0	0	0	10	20

*phr – parts per hundred rubber

The chemicals required for the composition were weighed and compounded using a two-roll mill to achieve uniform mixing. After a gap of one day, the processed rubber was cut into 90g pieces and then molded into 3 mm rubber sheets using a hydraulic press. Specimens were cut according to the requirement for various tests. Button samples were prepared from compounded rubber with button mold and were subjected to post-curing in a hot air oven at 80°C for 8 hours.

2.3 Hardness Test

The hardness test was carried out on right cylindrical button samples of 12 mm thickness and with a diameter of 28 mm. Hardness was measured using a durometer hardness tester (BSE SHR-A) on the Shore-A scale according to the ASTM D2240 standard. The durometer probe was pressed at five different locations on each flat side of the button samples, and the values were averaged.

2.4 Tensile Testing

The tensile test was conducted using a universal testing machine (UTM) (Model UTB9251Dak system Inc., India) with 5 samples of each composition according to the ASTM D412 - C standard as per the dimensions shown in Fig. 1.

The samples were loaded onto the tensile testing machine and extended at a cross-head speed of 50 mm/min and performed till the samples were broken. The respective travel/elongation was recorded using the software.

The vibration test was conducted on a scale model (1:2 ratio) of a truck chassis, as shown in Fig. 2.

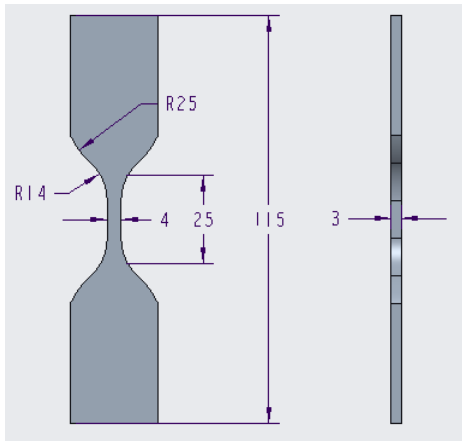


Figure 1: ASTM D412 - Dog-bone specimen dimensions

2.5 Test for Damping Properties

The chassis is made of sections of mild steel channels welded together and machined to suit the need. The chassis supported on two stands kept on the floor was subjected to forced vibration using an electric motor fastened on top of it. An accelerometer mounted on the chassis was used to measure the resulting vibration. The compounded rubber sheets were packed in between the electric motor and chassis to study its damping effect, as shown in Fig. 3.

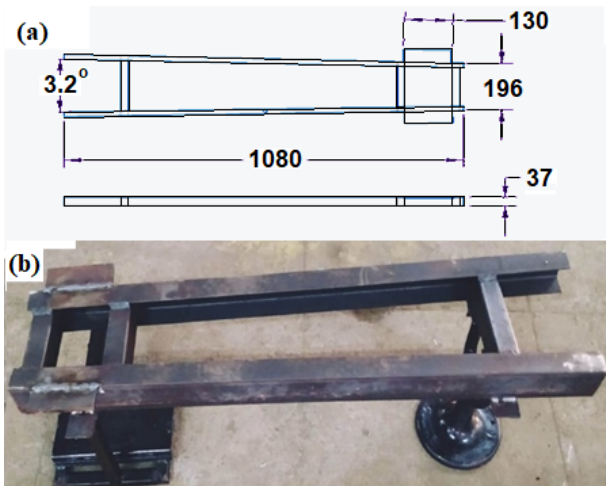


Figure 2: (a) Chassis dimensions; (b) Fabricated chassis

First, the vibration value without any damping was recorded for reference. Then the experiment was repeated with different composite samples as a damping medium. The collected vibration data was exported into an Excel file using a Data Acquisition System (DAQ) module, interfaced with a computer running a MATLAB program.

A tri-axial accelerometer from KISTLER (Model No. 8763B500BB) with a range of $\pm 500g$ and 10 mV/g sensitivity was interfaced with NI 9234 4-channel compact DAQ hardware.

Table 2: Mechanical properties

SAMPLES	Hardness Shore A	Tensile strength (MPa)	Elongation at break (%)	M100 (MPa)	Stiffness @100% (kN/m)
SBR Blank	54 \pm 1	1.10 \pm 0.04	136.67 \pm 6	0.91 \pm 0.03	0.439 \pm 0.01
SBR 10 CB	58 \pm 1	2.96 \pm 0.11	342.36 \pm 28	1.03 \pm 0.03	0.496 \pm 0.01
SBR 20 CB	62 \pm 1	3.32 \pm 0.05	428.98 \pm 11	1.26 \pm 0.04	0.607 \pm 0.02
SBR 10 GNP	59 \pm 1	2.55 \pm 0.2	347.77 \pm 19	1.26 \pm 0.05	0.606 \pm 0.03
SBR 20 GNP	63 \pm 1	2.77 \pm 0.2	398.15 \pm 20	1.45 \pm 0.09	0.700 \pm 0.04

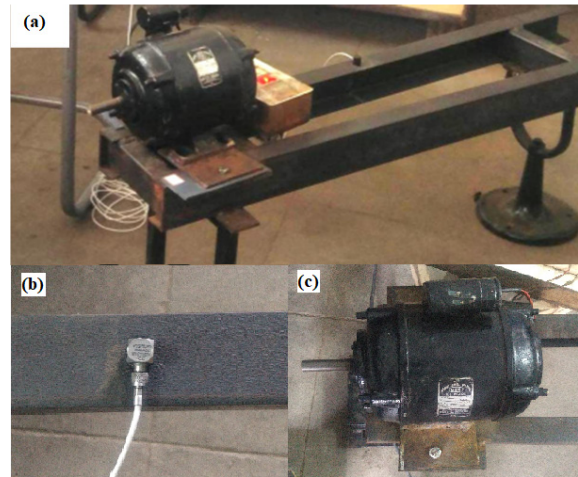


Figure 3: (a) Assembled model; (b) Accelerometer; (c) Motor/Vibration source

3. RESULTS AND DISCUSSION

3.1 Mechanical Properties

The characteristics of mechanical properties of graphene and carbon black composites are presented in Table 2. The most prominent mechanical test is hardness testing. The Shore A hardness was measured in this case, and it increases with an increase in filler content. Graphene leads in this parameter against carbon black. This is mainly attributed to cross-linking of the nanofiller being greater than that of micro carbon black due to increased contact and smaller particle size, resulting in better hardness of graphene samples.

The tensile test reveals an increase in tensile strength when the fillers are added to the neat SBR. The rise in tensile strength seems to be in proportion to the volume fraction of filler particles added to the base rubber. This indicates good dispersion of filler material with the SBR base, and also, the interfacial interaction between the layers is well developed. The GNP serves as an excellent reinforcing element among the fillers as it increases the elongation, modulus, and stiffness with the increase in filler proportion. As a result of the nanofiller's ability to transfer stress from the matrix, the modulus at 100% increases rapidly with the addition of GNPs [35]. Furthermore, graphene can function as a physical crosslinking spot, improving the modulus even more [36]. At the same time, the stiffness of the SBR is not enhanced as effectively with the introduction of carbon black. With the same filler content (10 phr), the stiffness of carbon black SBR composite (0.496 kN/m) is improved only by 13% from the neat SBR (0.439 kN/m), whereas the sample reinforced with GNP (0.606 kN/m) showed 38% improvement, which the sample with CB content (20 phr) could just match.

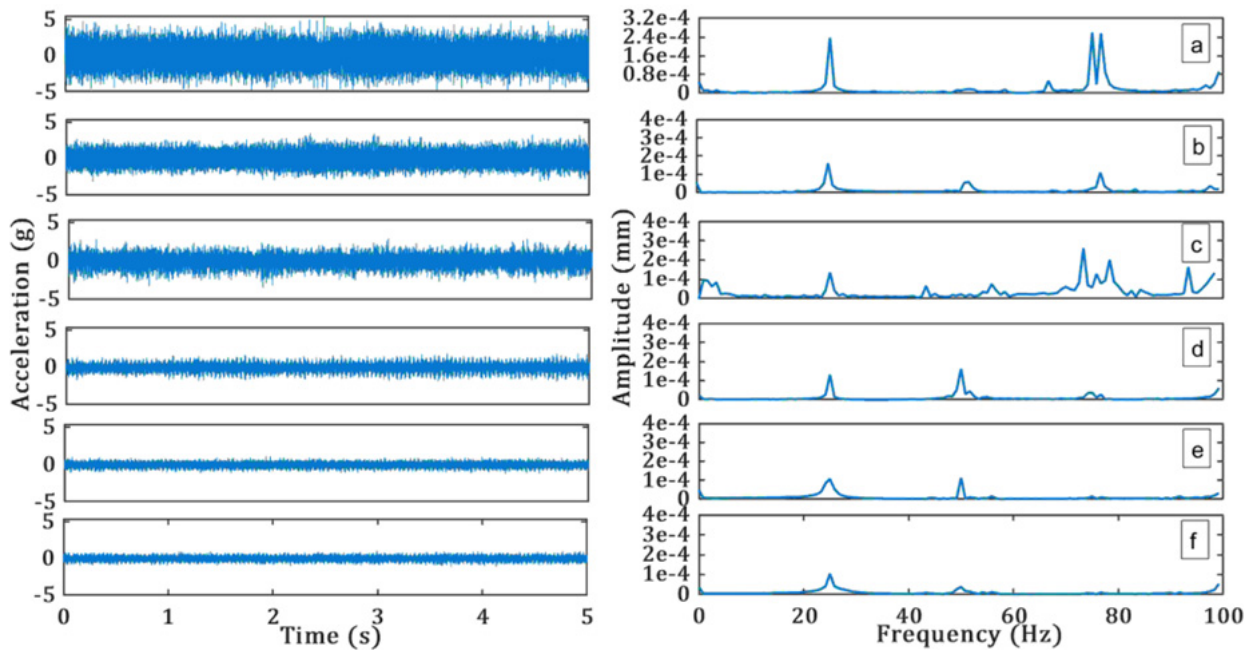


Figure 4. Experimental vibration data: (a) Undamped system; (b) SBR Blank; (c) SBR 10 CB; (d) SBR 20 CB; (e) SBR 10 GNP; (f) SBR 20 GNP

3.2 Vibration Analysis

The increase in stiffness proves the enhancement of damping properties. The vibration analysis was conducted on the chassis model, and the damping for the same was conducted by involving the SBR composite as a damping material. As the sample with higher phr GNP proved to be better, values of the same are shown in Fig. 4 for blank SBR and undamped conditions.

The excitation frequency from the vibrating system was found to be 25Hz, and the experiment was conducted for the same. The undamped system, i.e., without any rubber padding, had an amplitude of 2.59×10^{-4} mm, and when the neat SBR composite sheet was added to absorb vibration, the amplitude came down to 1.29×10^{-4} mm. It was further reduced to 1.17×10^{-4} mm and 1.14×10^{-4} mm with SBR 10 CB and SBR 20 CB, respectively. In contrast, the amplitude lowered to 1.12×10^{-4} mm and 1.09×10^{-4} mm with SBR 10 GNP and SBR 20 GNP, respectively.

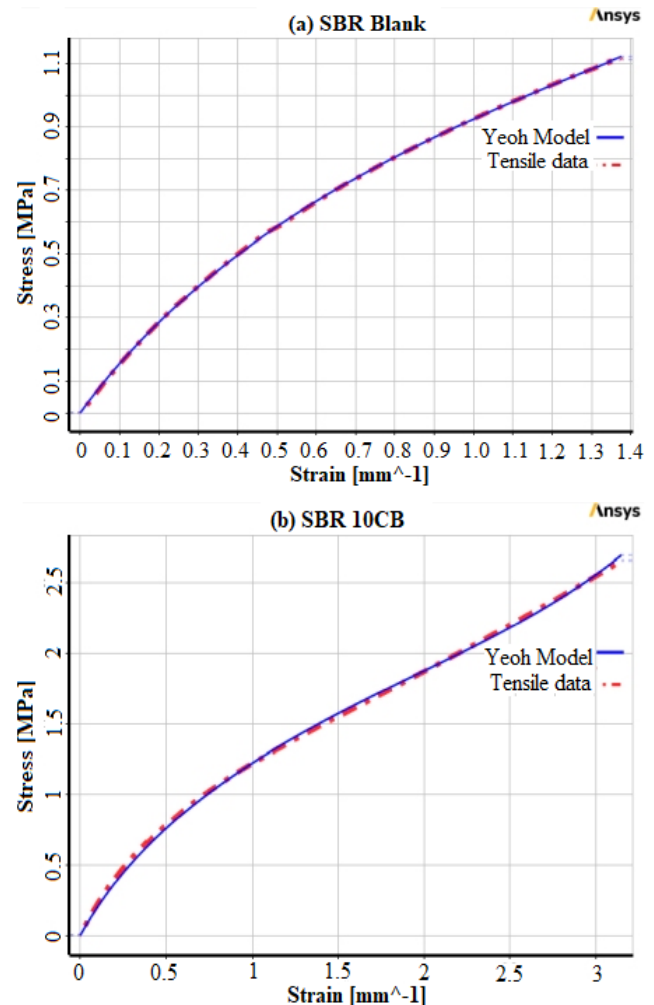
The samples displaying higher stiffness values in the tensile testing have proven to be more effective in attenuating the vibrations, hence proving to be more desirable for damping material. As the natural frequency of a vibrating body greatly depends on the material stiffness, GNP filler added SBR is more desirable.

The addition of fillers has increased the mechanical characteristics of the rubber composites, resulting in a considerable increase in both the mechanical and vibrational properties of the composite over its blank form.

3.3 Ansys Validation - Tensile test

The tensile strength value acquired from the experiment was used to create a numerical model within Ansys Material Library, and new material was introduced. And this material was used to replicate the function of the damping layer, and the accuracy was validated successfully.

Yeoh's 3rd-order model was used for creating a hyper-elastic material in the Ansys Material library. A separate model was created for each test case, namely, SBR Blank, SBR 10 CB, SBR 20 CB, SBR 10 GNP, and SBR 20 GNP.



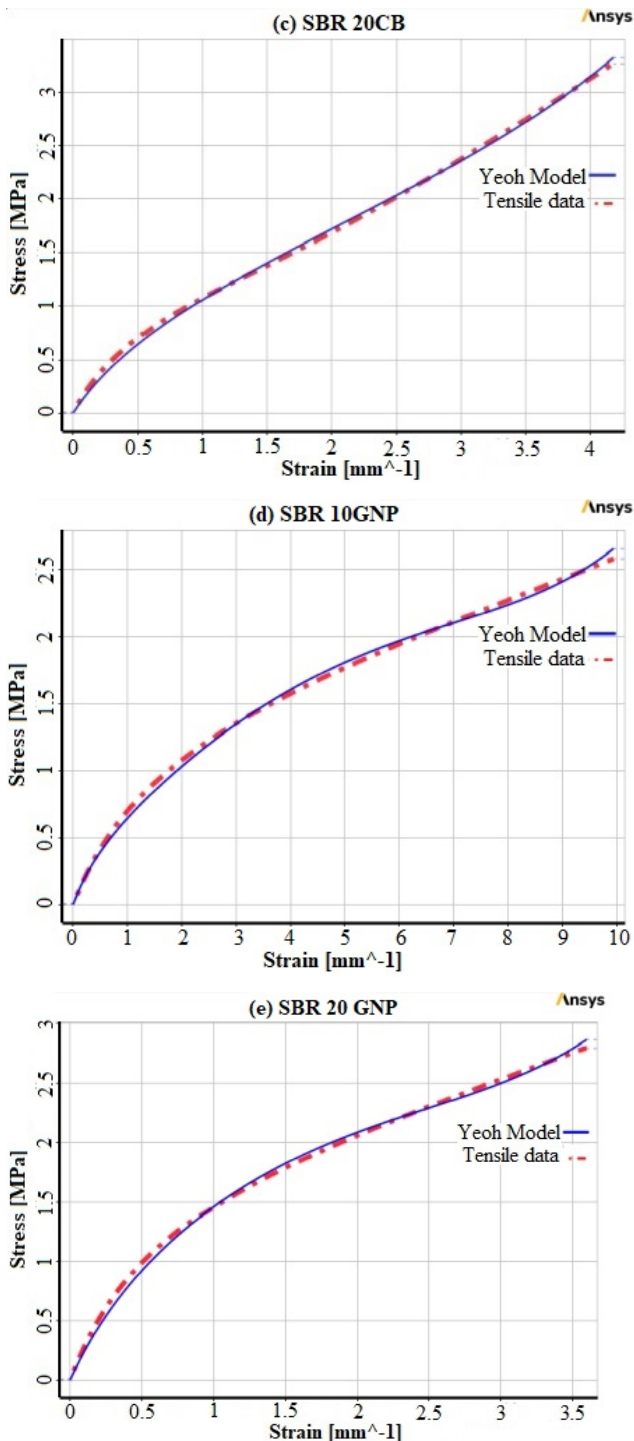


Figure 5: Yeoh 3rd Order curve fit; (a) SBR; (b) SBR10 CB; (c) SBR 20 CB (d) SBR10 GNP; (e) SBR 20 GNP

To analyze the hyperelastic model, the tensile stress-strain data of each sample was loaded, and these data were curve-fitted (refer to Fig. 5) to obtain the material constants. The “Absolute error” norm was used to calculate the material constants and is listed in the table. 3

Table 4: Reaction Force and Stress from Ansys

Elongation (mm)	SBR Blank		SBR 10 GNP		SBR 20 GNP		SBR 10 CB		SBR 20 CB	
	Force (N)	Stress (Mpa)	Force (N)	Stress (Mpa)	Force (N)	Stress (Mpa)	Force (N)	Stress (Mpa)	Force (N)	Stress (Mpa)
5	3.4923	0.2910	5.0227	0.41856	6.2980	0.5248	4.8657	0.4054	4.4145	0.3678
10	6.0822	0.5068	8.4071	0.7005	10.3887	0.8657	8.0245	0.6687	7.28883	0.6074
15	8.0638	0.67198	10.9381	0.9115	13.4200	1.1183	10.6536	0.8878	9.4077	0.7839
20	9.6726	0.8060	12.9590	1.0799	15.8529	1.3210	12.7922	1.0660	11.2618	0.9384

Table 3: Yeoh Parameters – Material Constant

SAMPLES	Yeoh, 3 rd Order (Mpa)		
	C10	C20	C30
SBR Blank	0.284264	-0.00587	0.000319
SBR 10 CB	0.366029	-0.00466	0.000155
SBR 20 CB	0.306269	-0.001	3.71E-05
SBR 10 GNP	0.18709	-0.00064	2.05E-06
SBR 20 GNP	0.447115	-0.0081	0.000163

After the material was created, a tensile test was simulated. For this reason, a dog-bone-shaped specimen of the ASTM D412 standard was generated using Creo software.

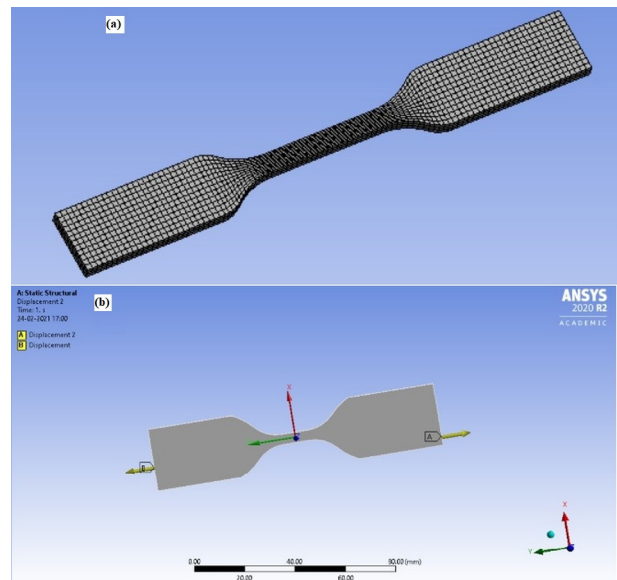


Figure 6: Tensile Test Pre-processing; (a) Meshing; (b) Boundary Conditioning

The model was imported into Ansys Workbench for performing the tensile test. From the convergence test, it was observed that there was no change in the results beyond 3744 elements having 20003 nodes. Meshed image is shown in Fig. 6. (a) & 6. (b) shows the boundary conditions and constraints.

Then the tensile test was successfully simulated for SBR blank, SBR 10 CB, SBR 20 CB, SBR 10 GNP, and SBR 10 GNP samples for four test cases, namely 5, 10, 15, and 20 mm of elongation given as input displacement. The output parameters are tabulated in Table.4.

Likewise, the tensile test carried out in Ansys was proved to be in satisfaction with the experimental result, the stress value attained from the Ansys, and the experiment had an average difference of 2e-02 MPa, as in fig. 7. Hence validating the tensile strength test. The Yeoh Hyper-Elastic model has been proven to be more accurate for rubber nano-composite materials having high elongation.

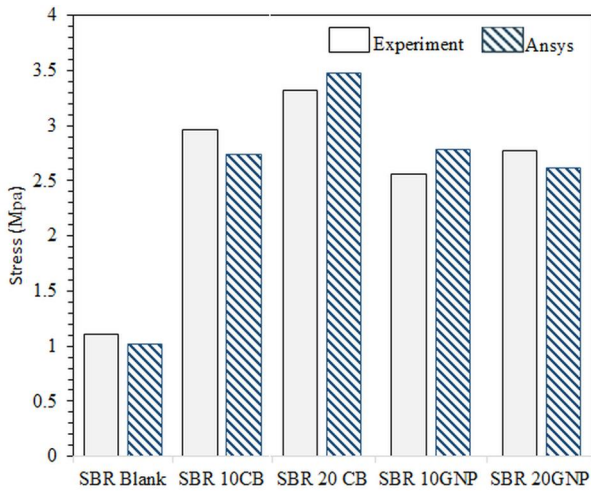


Figure 7: Tensile test error

From this simulation, it is evident that the addition of GNP to SBR increases the stress induced in the body, which implies improved stiffness value.

3.4 Ansys Validation - Harmonic Analysis

To validate the vibrational experiment, harmonic response analysis was conducted in Ansys workbench. The material model used for tensile testing was imported into the module. The model was generated in Creo with the 1:1 scale to the Prototype model fabricated. Then the entire test setup was modeled and assembled Fig. 8.

This Assembled model was imported into the Ansys Workbench-Harmonic Response module and was meshed with 28227 elements, as shown in Fig. 9.

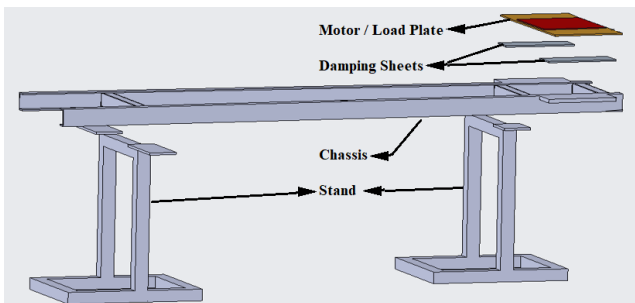


Figure 8: Set-up Creo Model

The excitation load was given over a plate to act as the motor, and the response frequency was recorded at a point 540 mm away from the excitation point, which resembles the accelerometer sensor.

The input frequency was calculated as follows;
 Speed of the Motor, $N = 1500 \text{ rpm}$
 Frequency, $f = N/60 = 1500/60 = 25 \text{ Hz}$ (constant)

Fig. 10 shows the amplitude response for different excitation frequencies, and the values of amplitudes are $2.4104\text{e-}4$, $1.3562\text{e-}4$, $1.22\text{e-}4$, $1.183\text{e-}4$, $1.1728\text{e-}4$ and $1.1321\text{e-}4$ for the undamped system, SBR blank, SBR 10 CB, SBR 20 CB, SBR 10 GNP, and SBR 20 GNP respectively, corresponding to input excitation frequency 25Hz.

The test error between the experimental values and simulated output is shown in Fig. 11; it can be seen that

there is negligible / no error in computed values. This indicates successful validation of the result.

Hence, to validate the experimental data. This proves the increase in stiffness and hence the modulus due to the addition of GNP in the SBR composite has increased the damping properties of the composite.

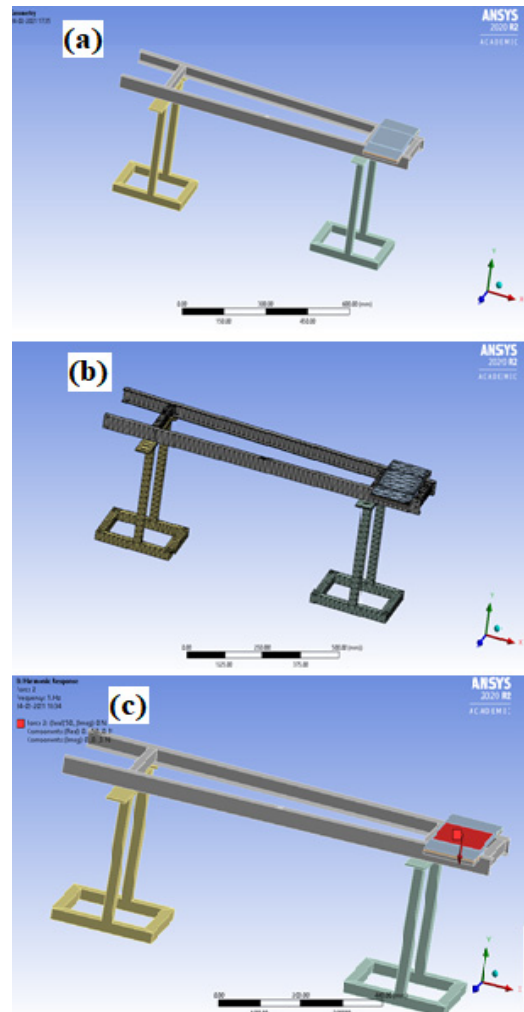
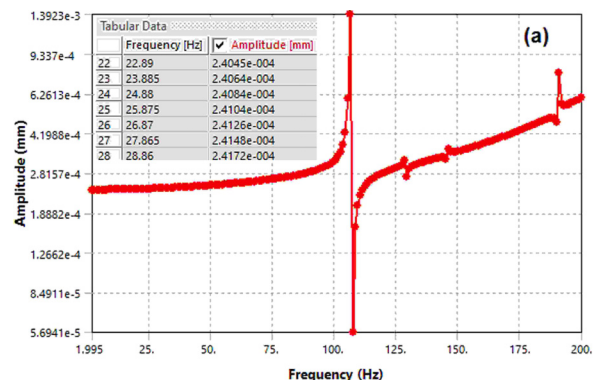


Figure 9: Harmonic response pre-processing; (a) Generated set-up; (b) Meshing; (c) Boundary conditions

3.5 SEM Imaging

Graphene nanoplatelets loaded at 10 phr in the SBR matrix are distributed evenly in the rubber matrix with little or no cluster formation that leads to exfoliated/intercalated composites. This could be evident from Fig. 12 (a).



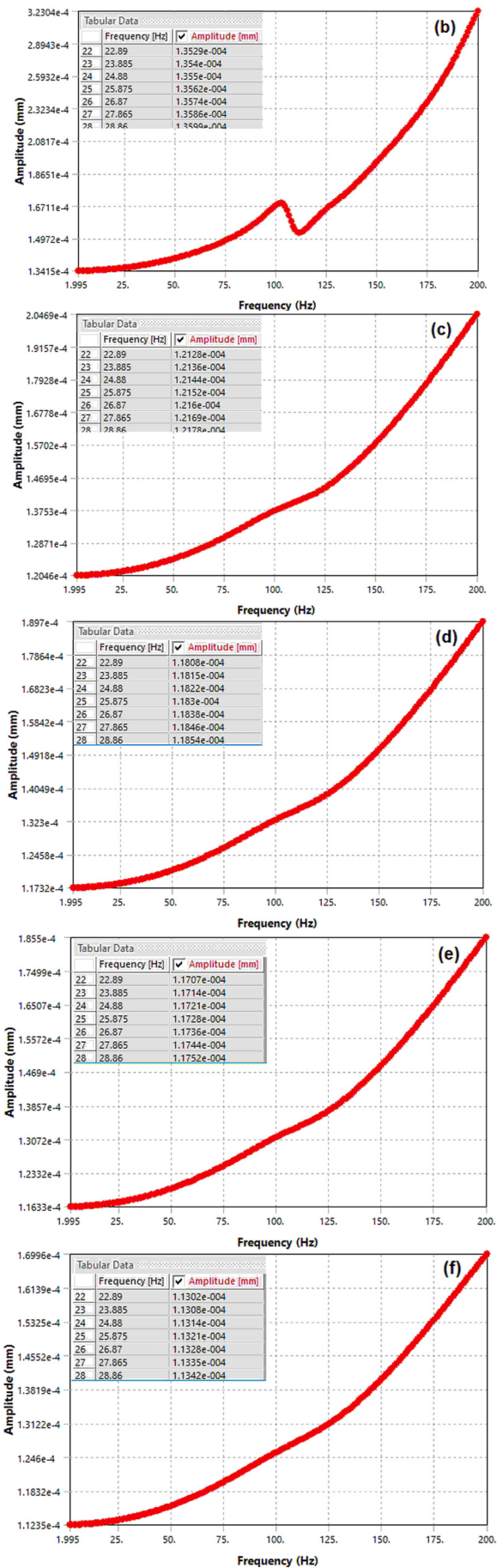


Figure 10: Ansys results; (a) Undamped system; Damped with (b) blank SBR; (c) SBR 10 CB (d) SBR 20 CB (e) SBR 10 GNP (f) SBR 20 GNP

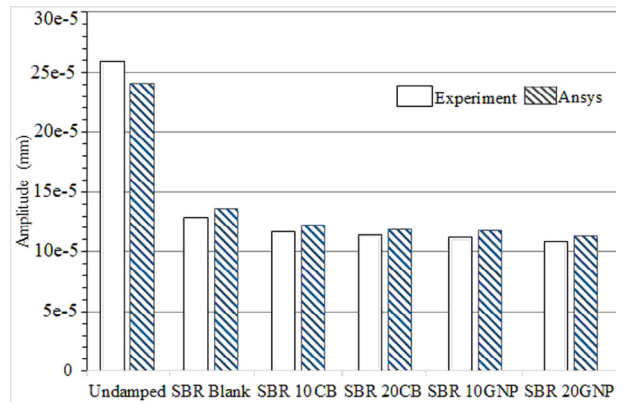
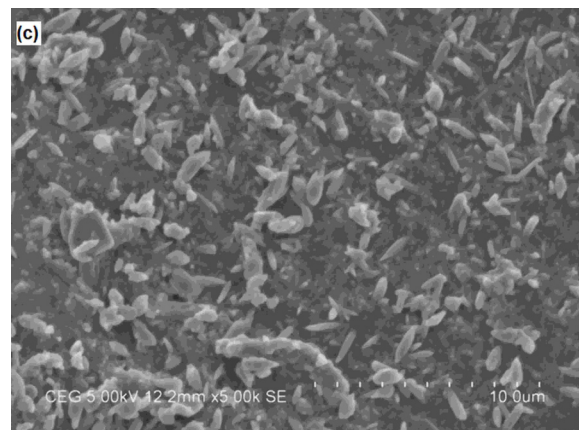
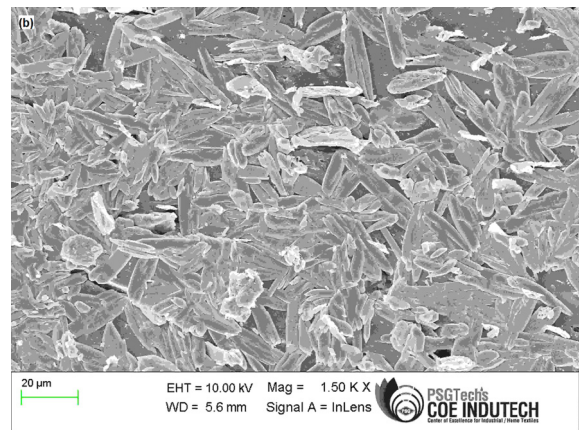
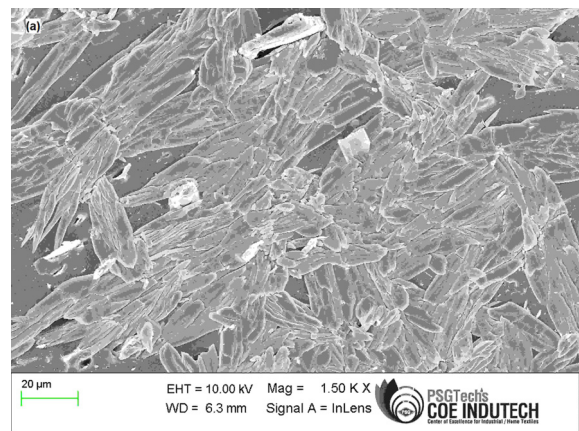


Figure 11: Vibration Test Error

However, when the filler proportion is increased to 20 phr, due to the high surface energy of GNP, more clusters were evident, which resulted in more filler-filler interactions (Figure 12 (b)).



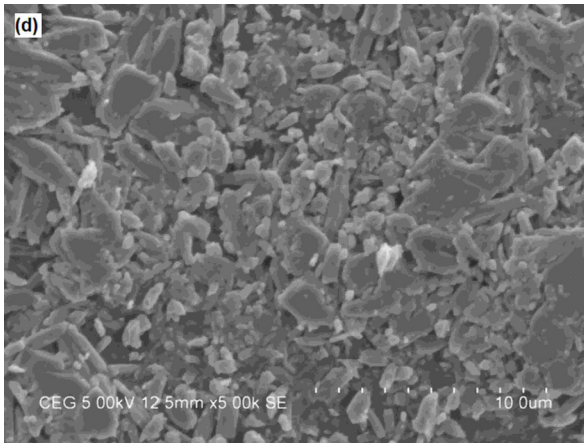


Figure 12: SEM images; (a) SBR 10 GNP; (b) SBR 20 GNP (c) SBR 10 CB (d) SBR 20 CB

4. CONCLUSION

The application of a rubber composite incorporating SBR and graphene reinforcement as a motor mount can offer exceptional vibration isolation, reducing the transfer of vibrations caused by the motor to the surrounding structure. This results in enhanced ride comfort and decreased noise levels in vehicles or equipment. The mechanical and damping properties of the SBR composites, reinforced with both carbon black (CB) and graphene nanoplatelets (GNP), were investigated to assess their performance. Investigations were carried out to see how factors such as filler type and composition affected performance. It was found that the addition of fillers had a positive effect on the mechanical properties of the base SBR. For the same volume composition, CB-filled composite has higher strength and ductility than GNP-filled composite. At the same time, the GNP composites showed better stiffness and improvement in hardness than the CB-loaded SBR.

Moreover, it was observed that graphene was a better option for reinforcement for damping enhancement. When compared to a blank SBR, damping increased by up to 84% when 20 Phr GNP was used. The results were validated in Ansys using Harmonic response analysis, which had a negligible error in comparison with experimental data. SBR composites with nanofillers may pave the way for the emergence of high-performance damping materials for various applications.

REFERENCES

[1] Dimitrios G. Papageorgiou, Ian A. Kinloch, Robert J. Young.: Mechanical properties of graphene and graphene-based nanocomposites, *Progress in Materials Science*, Vol. 90, 2017

[2] A. Mostafa, A. Abouel-Kasem, M.R. Bayoumi, M.G. El-Sebaie.: Insight into the effect of CB loading on tension, compression, hardness and abrasion properties of SBR and NBR filled compounds, *Materials & Design*, Vol. 30, No. 5, pp. 1785-1791, 2009

[3] Xiangwen Zhou, Yuefeng Zhu, Qianming Gong, Ji Liang.: Preparation and properties of the powder SBR composites filled with CNTs by spray drying

process, *Materials Letters*, Vol. 60, No. 29–30, pp. 3769-3775, 2006

[4] Xiaodong Xue, Qing Yin, Hongbing Jia, Xuming Zhang, Yanwei Wen, Qingmin Ji, Zhaodong Xu.: Enhancing mechanical and thermal properties of styrene-butadiene rubber/carboxylated acrylonitrile butadiene rubber blend by the usage of graphene oxide with diverse oxidation degrees, *Applied Surface Science*, Vol. 423, pp. 584-591, 2017

[5] Xiang-Wen Zhou, Yue-Feng Zhu, Ji Liang.: Preparation and properties of powder styrene-butadiene rubber composites filled with carbon black and carbon nanotubes, *Materials Research Bulletin*, Vol. 42, No. 3, pp. 456-464, 2007

[6] Yanping Wu, Lei Chen, Jinlong Li, Huidi Zhou, Haichao Zhao, Jianmin Chen.: Understanding the mechanical and tribological properties of solution styrene butadiene rubber composites based on partially graphene oxide, *European Polymer Journal*, Vol. 89, pp. 150-161, 2017

[7] J.Y. Wang, H.B. Jia, Y.Y. Tang, D.D. Ji, Y. Sun, X.D. Gong, L.F. Ding.: Enhancements of the mechanical properties and thermal conductivity of carboxylated crylonitrile butadiene rubber with the addition of graphene oxide, *J. Mater. Sci.*, Vol.48, No. 4, pp. 1571-1577, 2013

[8] H.L. Kang, K.H. Zuo, Z. Wang, L.Q. Zhang, L. Liu, B.C. Guo.: Using a green method to develop graphene oxide/elastomers nanocomposites with combination of high barrier and mechanical performance, *Composites Science and Technology*, Vol. 92, pp. 1-8, 2014

[9] B. Yin, J. Wang, H. Jia, J. He, X. Zhang, Z. Xu.: Enhanced mechanical properties and thermal conductivity of styrene-butadiene rubber reinforced with polyvinylpyrrolidone-modified graphene oxide, *Journal of Materials Science*, vol. 51, pp. 5724-5737, 2016

[10] Liu, Z., Zhang, Y.: Enhanced mechanical and thermal properties of SBR composites by introducing graphene oxide nanosheets decorated with silica particles, *Composites: Part A*, 2017

[11] Leyu Lin, Nicholas Ecke, Sebastian Kamerling, Chong Sun, He Wang, Xiangyu Song, Kai Wang, Shugao Zhao, Jianming Zhang, Alois K. Schlarb.: Study on the impact of graphene and cellulose nanocrystal on the friction and wear properties of SBR/NR composites under dry sliding conditions, *Wear*, Vol. 414–415, pp. 43-49, 2018

[12] Li Z, Zhang J, Chen S.: Effects of carbon blacks with various structures on vulcanization and reinforcement of filled ethylene-propylene-diene rubber. *Express Polym Lett.*, vol. 2, No.10, pp. 695- 704, 2008

[13] P. Berki, R. Göbl, J. Karger-Kocsis.: Structure and properties of styrene-butadiene rubber (SBR) with pyrolytic and industrial carbon black, *Polymer Testing*, Vol. 61, 2017

[14] Sivakumar C, Muralidharan. V, N Ravikumar, Murali Manohar D.: Numerical Analysis on

Mechanical Behavior of Viscoelastic Nano Composite, SAE Technical Paper 2021-28-0240, 2021

- [15] Dharmaraj, M.M., Chakraborty, B.C. & Begum, S.: The effect of graphene and nanoclay on properties of nitrile rubber/polyvinyl chloride blend with a potential approach in shock and vibration damping applications. *Iran Polym J*, Vol. 31, pp. 1129–1145, 2022
- [16] Sun L, Gibson RF, Gordaninejad F, Suhr J.: Energy absorption capability of nanocomposites: A review. *Compos Sci Technol*, Vol. 69, No. 14, pp. 2392–2409, 2009
- [17] Bumyong Yoon, Ji Yeon Kim, Uiseok Hong, Min Kyeong Oh, Munsung Kim, Sang Bae Han, Jae-Do Nam, Jonghwan Suhr.: Dynamic viscoelasticity of silica-filled styrene-butadiene rubber/polybutadiene rubber (SBR/BR) elastomer composites, *Composites Part B: Engineering*, Vol. 187, 2020
- [18] E.C. Botelho, A.N. Campos, E. de Barros, L.C. Pardini, M.C. Rezende.: Damping behavior of continuous fiber/metal composite materials by the free vibration method, *Composites Part B: Engineering*, Vol. 37, No. 2–3, 2005
- [19] Himanshu Rajoria, Nader Jalili.: Passive vibration damping enhancement using carbon nanotube-epoxy reinforced composites, *Composites Science and Technology*, Vol. 65, No. 14, 2005
- [20] Dharmaraj, M.M., Chakraborty, B.C., Begum. S, Ravikumar. N, Sivakumar. C.: Effect of nanoclay reinforcing filler in nitrile rubber/polyvinyl chloride blend: frequency response of dynamic viscoelasticity and vibration damping, *Iran Polym J*, Vol. 31, pp. 1247–1261, 2022
- [21] E. Sarlin, Y. Liu, M. Vippola, M. Zogg, P. Ermanni, J. Vuorinen, T. Lepistö.: Vibration damping properties of steel/rubber/composite hybrid structures, *Composite Structures*, Vol. 94, No. 11, 2012
- [22] Jinshui Yang, Jian Xiong, Li Ma, Bing Wang, Guoqi Zhang, Linzhi Wu.: Vibration and damping characteristics of hybrid carbon fiber composite pyramidal truss sandwich panels with viscoelastic layers, *Composite Structures*, Vol. 106, 2013
- [23] Shao Hui Zhang, Hua Ling Chen.: A study on the damping characteristics of laminated composites with integral viscoelastic layers, *Composite Structures*, Vol. 74, No. 1, 2006
- [24] J.S. Moita, A.L. Araújo, C.M. Mota Soares, C.A. Mota Soares.: Finite element model for damping optimization of viscoelastic sandwich structures, *Advances in Engineering Software*, Vol. 66, 2013
- [25] Pöschl, Marek, Martin Vašina, Petr Zádrapa, Dagmar Měřínská, and Milan Žaludek.: Study of Carbon Black Types in SBR Rubber: Mechanical and Vibration Damping Properties, *Materials*, Vol. 13, No. 10: 2394, 2020, <https://doi.org/10.3390/ma13102394>
- [26] Roja Esmaeeli, Siamak Farhad.: Parameters estimation of generalized Maxwell model for SBR and carbon-filled SBR using a direct high-frequency DMA measurement system, *Mechanics of Materials*, Vol. 146, 2020
- [27] Wei Sun, Xianfei Yan & Feng Gao.: Analysis of frequency-domain vibration response of thin plate attached with viscoelastic free layer damping, *Mechanics Based Design of Structures and Machines*, Vol. 46, No. 2, pp. 209–224, (2018), DOI: 10.1080/15397734.2017.1327359
- [28] Gianmarco Vergassola, Dario Boote & Angelo Tonelli.: On the damping loss factor of viscoelastic materials for naval applications, *Ships and Offshore Structures*, Vol. 13, No. 5, pp. 466–475, 2018 DOI: 10.1080/17445302.2018.1425338
- [29] Bhudolia, S.K., Perrotey, P., Joshi, S.C., Enhanced Vibration damping and dynamic mechanical characteristics of composites with novel pseudo-thermoset matrix system, *Composite Structures*, Vol. 179, pp. 502–513, 2017
- [30] Garinis, D., Dinulović, M., Rašuo B.: Dynamic analysis of modified composite helicopter blade, *FME Transactions*, Vol. 40, No.2, pp. 63–68, 2012
- [31] Dinulović, M., Rašuo, B., Trninić, MR., Adžić, VM.: Numerical Modeling of Nomex Honeycomb Core Composite Plates at Meso Scale Level, *FME Transactions* Vol. 48, No. 4, pp. 874–881, 2020. doi:10.5937/fme2004874D
- [32] Dinulović, M., Rašuo, B., Slavković, A., Zajić, G.: Flutter Analysis of Tapered Composite Fins: Analysis and Experiment, *FME Transactions*, Volume 50, No. 3, pp. 576–585, 2022, doi: 10.5937/fme2203576D
- [33] M Dinulović, B Rašuo, N Slavković, Đ Karić, Analysis of Aspect and Taper Ratio on Aeroelastic Stability of Composite Shells, *FME Transactions*, Volume 50 No. 4, pp. 732–744, 2022, doi: 10.5937/fme2204732D
- [34] Rasuo, B.: Experimental study of structural damping of composite helicopter blades with different cores, *Plastics, Rubber and Composites*, Volume 39, Issue 1, 2010, doi: 10.1179/174328910X12608851832092
- [35] Young, R.J., Liu, M., Kinloch, I.A., Li, S., Zhao, X., Valles, C., Papageorgiou, D.: The mechanics of reinforcement of polymers by Graphene nanoplatelets. *Compos. Sci. Technol.* 2018
- [36] Araby, S., Zaman, I., Meng, Q., Kawashima, N., Michelmore, A., Kuan, H.-C., Majewski, P., Ma, J., Zhang, L.: Melt compounding with graphene to develop functional, high-performance elastomers. *Nanotechnology* 2013

NOMENCLATURE AND ABBREVIATIONS

f	Frequency
N	Speed of the Motor
SBR	Styrene-butadiene rubber
GNP	Graphene nanoparticles
CB	Carbon black
NBR	Nitrile rubber
NBR-PVC	Nitrile rubber/polyvinyl chloride

CNT	Carbon nanotubes
XNBR	Carboxylated acrylonitrile butadiene rubber
GO	Graphene oxide
NR	Natural rubber
CNC	Cellulose nanocrystal
EPDM	Ethylene-propylene-diene rubber
pCB	Pyrolytic carbon black
OMMT	Organically modified montmorillonite
DMA	Dynamic mechanical analyzer
CLD	Constrained layer damping
HFDMA	High-frequency dynamic mechanical analyzer
GMM	General maxwell mode
WLF	Williams, Landel and Ferry
MMA	Methylmethacrylate
ZnO	Zinc oxide
TMTD	Tetra methyl thiuram disulfide
phr	Parts per hundred rubber
UTM	Universal testing machine
DAQ	Data acquisition system

ИСТРАЖИВАЊА МЕХАНИЧКИХ И ПРИГУШУЈУЋИХ СВОЈСТАВА СТИРЕН-

БУТАДИЕН КАУЧУКА СА ГРАФЕНОМ И ЧАЊИ

К. Сивакумар, В. Муралидхаран, Н. Равикумар, Д. Мурали Манохар

У овом раду је приказано експериментално и нумеричко истраживање механичких и пригушујућих својстава композита стирен-бутадиен каучука (СБР) са наночестицама графена (ГНП) и чањом (ЦБ). Композити су тестирани на механичка својства као што су тврдоћа и затезна чврстоћа. Примећено је да композити са ГНП и ЦБ пунилина имају већу крутост и процентуално издуживање због лома. Модел шасије је подвргнут принудним вибрацијама да би се пронашла својства пригушења сваког од припремљених композита. Експериментални резултати су коришћени за креирање нумеричког модела у АНСИС софтверу користећи Иеох-ов хипереластичан модел за генерисање хипереластичног материјала за симулацију својстава композита и за извођење анализе хармонијског одзива у АНСИС-у. Резултати експеримената и теоријских налаза показали су добру сагласност.